Experimental and *ab initio* volume compressibility curves of $NpCoGa_5$

S. Heathman, P. Heines, S. Surblé, J.-C. Griveau, N. Magnani, and R. Caciuffo
European Commission, Joint Research Centre, Institute for Transuranium Elements, Postfach 2340, D-76125 Karlsruhe, Germany

S. Elgazzar* and P. M. Oppeneer
Department of Physics and Materials Science, Uppsala University, P.O. Box 530, S-751 21 Uppsala, Sweden
(Received 19 October 2009; revised manuscript received 15 December 2009; published 15 January 2010)

We report the results of high-pressure, angular-dispersive, x-ray diffraction measurements performed on $NpCoGa_5$, a magnetic isostructural analog of the $PuCoGa_5$ superconductor. No crystallographic transitions or discontinuous volume collapses have been observed by increasing pressure p up to 39 GPa. A fit to the Birch-Murnaghan equation of state gives values of the isothermal bulk modulus and its pressure derivative $B_0=130$ GPa and $B_0'=4.8$, respectively. The volume compressibility curve is in excellent agreement with the results of *ab initio* fully relativistic, full potential local spin-density-functional calculations. A comparison to experimental and *ab initio* calculated compressibility data of $PuCoGa_5$ and $PuRhGa_5$ is also made.

DOI: 10.1103/PhysRevB.81.024106 PACS number(s): 71.27.+a, 78.70.Nx, 75.30.Et

I. INTRODUCTION

A most intriguing issue of condensed-matter physics is the relation between unconventional superconductivity, magnetism, and non-Fermi-liquid behavior in proximity of a zero-temperature critical point separating phases of different symmetry. The series of isostructural RTX_5 intermetallic compounds containing cerium or a light actinide element R, a transition metal T (Fe, Co, Ni, Rh, or Ir), and an element of the boron group X (Ga or In), is an ideal playground for investigating such an issue. The members of the series feature a variety of unusual phenomena, from direct coupling of magnetic and superconducting order in $CeCoIn_5$ (Refs. 1 and 2) to high-temperature heavy-fermion superconductivity in $PuCoGa_5$.[3,4] Current models of superconductivity in these compounds involve magnetically mediated d-wave Cooper pairing of itinerant f electrons,[5,6] but the nature of the mediating bosons has not been firmly established.[4,7] In the case of $PuCoGa_5$, the formation of a novel condensate of composite pairs between local moments and electrons, with either d- or g-wave symmetry, has been recently proposed.[8]

RTX_5 compounds crystallize in the tetragonal $HoCoGa_5$-type structure (space group $P4/mmm$). The R atoms occupy the 1a positions, the T atoms are in the 1b positions (halfway between the R atoms along the c direction) and there are two crystallographic positions for the X atoms, one at the center of the basal planes (1c), and four at the 4i position, in the rectangular faces of the unit cell with reduced coordinates $(0,1/2,z)$ (see Fig. 1).

$NpCoGa_5$($a=4.277$ Å, $c=6.787$ Å, $z=0.3103$) is a magnetic member of the series, exhibiting a longitudinal-modulated antiferromagnetic (AF) order below $T_N \approx 47$ K, with an ordered Np moment $\mu=0.84\mu_B$ pointing along the tetragonal c axis.[9–11] The magnetic structure is defined by the propagation vector (0, 0, 1/2) and is shown in Fig. 1. The magnetic form factor has been measured by polarized neutron diffraction and is consistent with a Np^{3+} electronic state.[12] The microscopic magnetization agrees with that observed in bulk susceptibility measurements and the magnetic moment has spin and orbital contributions as expected for intermediate coupling. Recent NMR experiments[13] in the paramagnetic state indicate a crossover from localized behavior at high temperatures to itinerant magnetic properties below 100 K. Interestingly, the magnetic excitation spectrum investigated by inelastic neutron scattering suggests itinerant behavior in the antiferromagnetically ordered state.[14] Also, low-temperature de Haas–van Alphen data[15] were reasonably well explained by *ab initio* density-functional calculations,[16] which lends further support to the picture of itinerant $5f$ behavior.

In this paper we report the results of room-temperature, high-pressure, angular-dispersive, x-ray diffraction measurements performed on $NpCoGa_5$. The volume compressibility, the isothermal bulk modulus (B_0), and its pressure derivative (B_0') determined from the experiment are compared with the

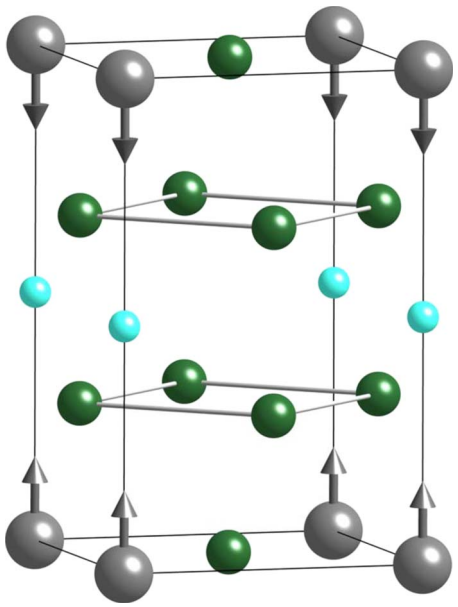

FIG. 1. (Color online) Crystal and magnetic structure of $NpCoGa_5$. Large (gray) spheres represent the Np atoms, small (cyan) and medium (green) smaller spheres represent Co and Ga atoms, respectively. The arrows indicate the direction of the Np magnetic moment in the AF phase below $T_N=47$ K.

results of *ab initio* local spin-density approximation (LSDA) calculations. The excellent agreement between experimental and theoretical data confirms that the adopted calculation scheme provides an accurate determination of the total energy of the system, and that the lattice parameters are well described assuming itinerant 5*f* states. In spite of this success, LSDA methods, with or without orbital polarization assumptions, do have a shortcoming for $NpCoGa_5$ in that these fail to reproduce the details of the antiferromagnetic properties.[16] We compare furthermore the results achieved for $NpCoGa_5$ to experimental and *ab initio* investigations of the compressibility of the isostructural actinide superconductors $PuCoGa_5$ and $PuRhGa_5$. The agreement between experimental and *ab initio* compressibility data is comparably good for $PuRhGa_5$, but somewhat poorer for $PuCoGa_5$. These findings indicate limitations of the LSDA itinerant 5*f* description for the Pu compounds.

II. EXPERIMENTAL DETAILS AND RESULTS

A polycrystalline sample of $NpCoGa_5$ was prepared by arc melting stoichiometric amounts of the constituent elements under an atmosphere of high-purity argon on a water-cooled copper hearth, using a Zr getter. Starting materials were used in the form of 3N8 cobalt and 3N7 gallium shot as supplied by A. D. Mackay Inc., and 3N neptunium metal. Homogeneity of the sample was ensured by turning over and remelting the button several times. Weight losses were below 0.5%. About 10 μg of material were loaded into a membrane-type diamond anvil cell (DAC), affording a maximum x-ray scattering angle $2\theta_{max} \approx 24°$. Diamond flats were of 300 μm diameter, and inconel gaskets of 150 μm (diameter) hole size and (indented) thickness 30 μm were used. To avoid the risk of contamination of any exterior part of the DAC by the Np-containing powder sample, the $NpCoGa_5$ powders were combined with a small amount of epoxy resin to form solid ("granular") pieces, which were loaded into the DAC. Silicone oil was used as pressure-transmitting medium. Pressure was calibrated by the ruby fluorescence method, using a single ruby ball of diameter smaller than 10 μm. Measurements were performed from ambient pressure up to 39 GPa with a rotating anode x-ray generator (Bruker) installed at ITU, Karlsruhe. X-ray wavelength and spot size at the sample position were 0.7094 Å(Mo $K\alpha_1$) and 100×100 μm^2. Diffraction images were recorded with a Bruker SMART Apex CCD (1024×1024 pixels of dimensions 61×61 μm^2). The DAC was rotated through a sample angle $\Delta\Omega = \pm 4°$ while collecting each diffraction pattern. The images were integrated using the ESRF FIT2D software,[17] which generates files suitable for profile refinement. The results of a similar experiment performed on Ce*T*Ga_5 and Pu*T*Ga_5(*T*=Co,Rh) are reported in Ref. 18.

Rietveld refinements were carried out using the FULLPROF package,[19] and a typical fit is shown in Fig. 2. Reliability factors were, in general, better than 5%. The derived crystallographic parameters were analyzed using two different methods. In the first one, the pressure variations in *a* and *c* are fitted to a polynomial quadratic in *p*,

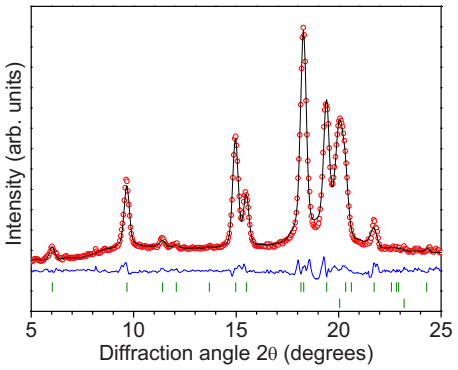

FIG. 2. (Color online) Diffraction pattern obtained for $NpCoGa_5$ by integrating Debye-Scherrer rings recorded with the area detector. The sample was at room temperature inside a membrane-type diamond anvil cell and submitted to a pressure of 1.3 GPa using silicone oil as pressure transmitting medium. Red circles represent experimental data, the solid black line is the refined Rietveld profile, vertical lines are reflection tick marks, and the lower blue line represents the difference profile.

$$a_i(p) = a_i(0) - k_i a_i(0) p + k_i' a_i(0) p^2, \tag{1}$$

where $i=1,2$, $a_1=a$, $a_2=c$, k_i and k_i' represent the linear compressibility along the lattice direction *i*. A rough estimate of the zero-pressure bulk modulus is then obtained as $B_0 = -\partial p / \partial \ln(V) = 1/(2k_a + k_c)$. The fits are shown by solid lines in Fig. 3, and give $k_a = 1.98 \times 10^{-3}$ GPa^{-1}, $k_a' = 1.3 \times 10^{-5}$ GPa^{-2}, $k_c = 1.95 \times 10^{-3}$ GPa^{-1}, and $k_c' = 1.13 \times 10^{-5}$ GPa^{-2} ($B_0 = 169$ GPa).

In the second method, B_0 and its pressure derivative B_0' are obtained by fitting the pressure-dependent relative volume $V(p)/V_0$ to the Birch and Murnaghan equation of state,[20–22]

$$p = \frac{3}{2} B_0 \left[\left(\frac{V}{V_0} \right)^{-7/3} - \left(\frac{V}{V_0} \right)^{-5/3} \right] \times \left\{ 1 + \frac{3}{4} (B_0' - 4) \left[\left(\frac{V}{V_0} \right)^{-2/3} - 1 \right] \right\}, \tag{2}$$

where *p* is the applied pressure, *V* is the volume, and V_0 is

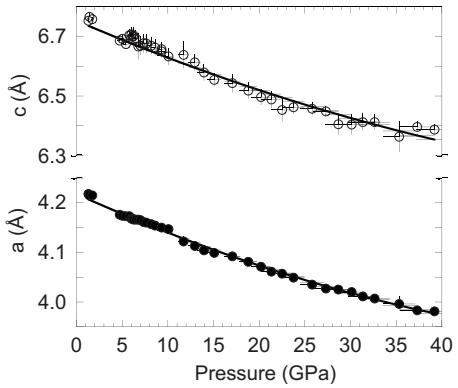

FIG. 3. Pressure dependence of the crystallographic lattice parameters of $NpCoGa_5$ at room temperature. The data have been obtained from the Rietveld refinement of the diffraction pattern. Solid lines are a fit to a quadratic polynomial as described in the text.

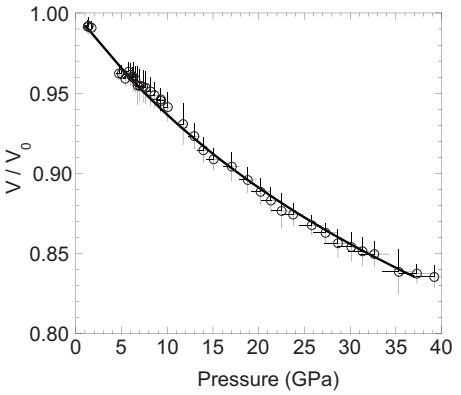

FIG. 4. Normalized unit-cell volume, $V(p)/V_0$ as a function of pressure for $NpCoGa_5$. The solid line is a fit to the Birch-Murnaghan equation of state.

the zero-pressure volume. The fit is shown by the solid line in Fig. 4 and gives $B_0=(130\pm 8)$ GPa and $B_0'=4.8\pm 0.5$.

III. *AB INITIO* CALCULATIONS AND COMPARISON WITH EXPERIMENTAL RESULTS

Ab initio density-functional theory calculations were performed with the relativistic version[23] of the full potential local orbital method.[24] In this scheme the four-component Kohn-Sham-Dirac equation, which implicitly contains spin-orbit coupling up to all orders, is solved self-consistently. The Perdew-Wang parametrization of the exchange-correlation potential in LSDA was used.[25] The adopted set of valence basis states was $5f$, $6s6p6d$, $7s7p$ for Np; $3d$, $4s4p$ for Co; and $3d$, $4s4p4d$ for Ga. The ground-state properties of $NpCoGa_5$ have been calculated assuming nonmagnetic (NM), ferromagnetic (FM), and antiferromagnetic ordered states (cf. Ref. 26). In the latter case, we considered both the experimentally determined AF1 structure with propagation vector (0, 0, 1/2) and the AF2 type of order characterized by a propagation vector (1/2, 1/2, 0) and realized in the isostructural compound $NpRhGa_5$.[11] For $PuCoGa_5$ we adopt the same set of basis functions, and for $PuRhGa_5$ we selected for Rh the $4d$ and $5s$, $5p$ basis states. Also, we assumed the same magnetic configurations as for $NpCoGa_5$, however, with the remark that magnetic ordering in $PuCoGa_5$ or $PuRhGa_5$ has thus far not been unambiguously detected.[12]

Total-energy calculations were performed as a function of volume, for a $12\times 12\times 12$ $\boldsymbol{k}$ mesh, corresponding to $196\boldsymbol{k}$ vectors in the irreducible wedge of the tetragonal Brillouin zone. The volume dependence of the cohesive energy $E(V)$ is then obtained from the total energies by subtracting isolated atom contributions.

The resulting total-energy curves are shown in the inset of Fig. 5. The equation of state at 0 K is finally calculated from the variation in the cohesive energy with respect to volume, $P=-\partial E/\partial V$, and is compared to experimental values in Fig. 5. We note that the experimental compressibility curves have been obtained at room temperature. The experimental volume differs therefore from the zero-temperature volume by the effect of the thermal expansion, a quantity which is not yet known for $NpCoGa_5$. In the comparison we hence ignore

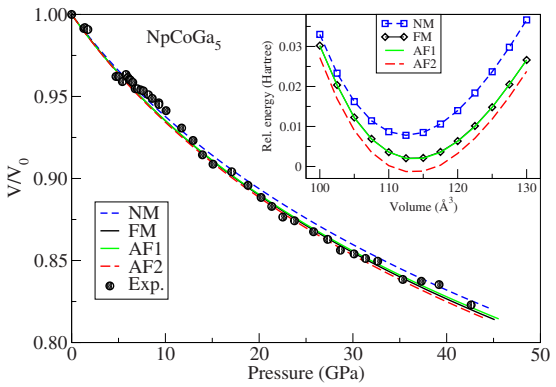

FIG. 5. (Color online) Comparison between experimental (filled circles) and *ab initio* calculated compression curves of $NpCoGa_5$. The calculated results are given for the nonmagnetic structure (blue dashed line, NM), ferromagnetic (black full line, FM), antiferromagnetic AF1 (green full line, AF1), and antiferromagnetic AF2 (red long-dashed line, AF2) types of orders. The calculated total-energy curves versus volume obtained for the investigated types of magnetic order are shown in the inset.

the influence of the thermal expansion. This is indeed a good approximation, because we consider the relative volume, $V(P)/V_0$, in which the thermal expansion is practically cancelled. Figure 5 shows that magnetic correlations do have a small, but non-negligible effect on the calculated compression curve. The best agreement is obtained when the experimentally observed magnetic structure is assumed. In this case, a fit of the theoretical curve to the Birch equation of state gives $B_0=124.9$ GPa and $B_0'=5.1$. It must be noticed, however, that the calculated magnetic ground-state structure is AF2, rather than AF1.[16]

Experimental compressibility data for the actinide superconductors $PuCoGa_5$ and $PuRhGa_5$ were reported recently.[18] To assess the compressibility behavior of these Pu-115 compounds in comparison to the Np analog, we plot in Fig. 6 experimental and *ab initio* calculated compressibility curves of the Pu-115's. The $V(p)$ curves were computed for the

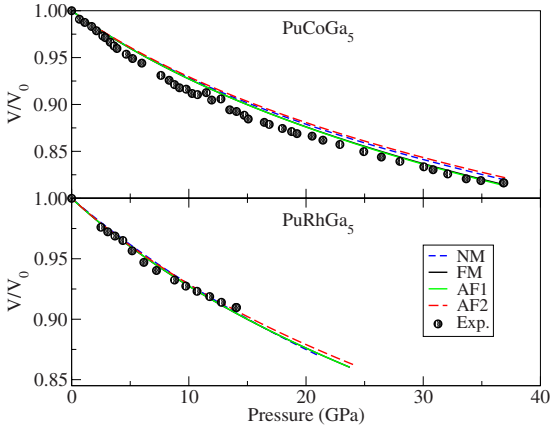

FIG. 6. (Color online) Comparison between experimental (circles) and *ab initio* calculated compression curves calculated for $PuCoGa_5$ (top panel) and $PuRhGa_5$ (bottom panel). The *ab initio* calculated compressibility curves are given for the NM, FM, antiferromagnetic AF1, and antiferromagnetic AF2 types of ordering.

same four magnetic structures as adopted for $NpCoGa_5$. The computed total energies versus unit-cell volume were reported in earlier studies.[27,26] As Fig. 6 shows the experimental compressibility curve of $PuRhGa_5$ is reasonably well explained by *ab initio* LSDA calculations. The computed curves for the various magnetic structures are rather close to one another, hence, it cannot be decided which magnetic structure provides the best agreement with the experimental data. The results for $PuCoGa_5$ give a different picture: the agreement between experiment and *ab initio* calculations is poorer, especially for pressures between about 5 and 20 GPa. The experimental data show a down turn in the $V(p)$ curve at about 5 GPa (see Fig. 6), thus evidencing a softening with pressure, which is not given by the *ab initio* calculation. There could be several explanations for this deviation. First, it could be that the itinerant treatment of the Pu $5f$ states, as embodied in the LSDA, does not sufficiently capture the nature of the $5f$ states of $PuCoGa_5$. It has been emphasized that the addition of a Coulomb U of about 3 eV improves the description and, in particular, reduces the magnetic moment on the Pu ion.[28,29] An influence of the pressure transmitting medium (oil) is an alternative possibility.[18] A freezing of the medium occurs for pressures above 10 GPa, which could influence the measurements.[18] A third reason, possibly also connected to the freezing of the medium, is that a difference in the pressure dependence of the a- and c-axis lattice parameters was observed. In the *ab initio* simulations shown in Fig. 6, however, a fixed c/a ratio was used, which is a suitable assumption for $NpCoGa_5$ (see Fig. 3). However, even with an influence of the pressure medium present, it appears that experimental and computed compressibility curves start to deviate already before the medium freezes, which would thus indicate some limitation of the $5f$ itinerant LSDA description to $PuCoGa_5$.

The compressibility data obtained for the three actinide-115 compounds is summarized in Table I. The good agreement between experiment and *ab initio* LSDA calculations is immediately apparent for $NpCoGa_5$. The trend of a smaller bulk modulus for $PuCoGa_5$ than for $PuRhGa_5$ is also reproduced in the calculations. However, the agreement with the experimental values is not as good as for $NpCoGa_5$. A previous calculation,[30] using the generalized gradient approximation, obtained a bulk modulus of 87 GPa for $PuCoGa_5$, in better agreement with experiment. This indicates that the gradient correction to the exchange-correlation functional explains the compressibility of $PuCoGa_5$ better than the standard local-density approximation.

TABLE I. Comparison of experimental and *ab initio* calculated bulk modulus (B_0) and its pressure derivative (B_0') of $NpCoGa_5$, $PuCoGa_5$, and $PuRhGa_5$.

	Experiment		Theory	
	B_0 (GPa)	B_0'	B_0 (GPa)	B_0'
$NpCoGa_5$	130 ± 8	4.8 ± 0.5	125	5.1
$PuCoGa_5$	89 ± 6	5.0	100	4.3
$PuRhGa_5$	104 ± 6	5.0	116	4.2

IV. CONCLUSION

In conclusion, the structural behavior of $NpCoGa_5$ under pressure has been studied by high-pressure x-ray diffraction and first-principles density-functional calculations in LSDA approximation. No crystallographic transitions or discontinuous volume collapses have been observed up to 41 GPa. The excellent agreement between experimental and calculated compression curves demonstrates that the adopted calculational scheme provides an accurate estimate of the cohesive energy of the system by assuming itinerant $5f$ electron states, although magnetic correlation effects are not completely captured.

ACKNOWLEDGMENTS

We thank J. Rebizant and D. Bouëxière for providing the sample used in this experiment. The high-purity neptunium metal required for the fabrication of the sample was made available through a loan agreement between Lawrence Livermore National Laboratory and ITU, in the frame of a collaboration involving LLNL, Los Alamos National Laboratory, and the U.S. Department of Energy. P.H., S.S., and N.M. acknowledge the European Commission for support in the frame of the Training and Mobility of Researchers program. Support from the Swedish Research Council (VR), JRC-ITU, and from the Swedish National Infrastructure for Computing (SNIC) is also acknowledged.

*On leave from Faculty of Science, Menoufia University, Shebin El-kom, Egypt.

[1] M. Kenzelmann, Th. Strässle, C. Niedermayer, M. Sigrist, B. Padmanabhan, M. Zolliker, A. D. Bianchi, R. Movshovich, E. D. Bauer, J. L. Sarrao, and J. D. Thompson, Science **321**, 1652 (2008).

[2] A. D. Bianchi, M. Kenzelmann, L. DeBeer-Schmitt, J. S. White, E. M. Forgan, J. Mesot, M. Zolliker, J. Kohlbrecher, R. Movshovich, E. D. Bauer, J. L. Sarrao, Z. Fisk, C. Petrović, and M. Ring Eskildsen, Science **319**, 177 (2008).

[3] J. L. Sarrao, L. A. Morales, J. D. Thompson, B. L. Scott, G. R. Stewart, F. Wastin, J. Rebizant, P. Boulet, E. Colineau, and G. H. Lander, Nature (London) **420**, 297 (2002).

[4] N. J. Curro, T. Caldwell, E. D. Bauer, L. A. Morales, M. J. Graf, Y. Bang, A. V. Balatsky, J. D. Thompson, and J. L. Sarrao, Nature (London) **434**, 622 (2005).

[5] P. Monthoux and G. G. Lonzarich, Phys. Rev. B **66**, 224504 (2002).

[6] P. Monthoux, D. Pines, and G. G. Lonzarich, Nature (London) **450**, 1177 (2007).

[7] F. Jutier, G. A. Ummarino, J.-C. Griveau, F. Wastin, E. Colineau, J. Rebizant, N. Magnani, and R. Caciuffo, Phys. Rev. B **77**,

024521 (2008).
[8] R. Flint, M. Dzero, and P. Coleman, Nat. Phys. **4**, 643 (2008).
[9] E. Colineau, P. Javorský, P. Boulet, F. Wastin, J. C. Griveau, J. Rebizant, J. P. Sanchez, and G. R. Stewart, Phys. Rev. B **69**, 184411 (2004).
[10] N. Metoki, K. Kaneko, E. Colineau, P. Javorský, D. Aoki, Y. Homma, P. Boulet, F. Wastin, Y. Shiokawa, N. Bernhoeft, E. Yamamoto, Y. Ōnuki, J. Rebizant, and G. H. Lander, Phys. Rev. B **72**, 014460 (2005).
[11] B. Detlefs, S. B. Wilkins, R. Caciuffo, J. A. Paixao, K. Kaneko, F. Honda, N. Metoki, N. Bernhoeft, J. Rebizant, and G. H. Lander, Phys. Rev. B **77**, 024425 (2008).
[12] A. Hiess, A. Stunault, E. Colineau, J. Rebizant, F. Wastin, R. Caciuffo, and G. H. Lander, Phys. Rev. Lett. **100**, 076403 (2008).
[13] H. Sakai, S. Kambe, Y. Tokunaga, T. Fujimoto, R. E. Walstedt, H. Yasuoka, D. Aoki, Y. Homma, E. Yamamoto, A. Nakamura, Y. Shiokawa, and Y. Ōnuki, Phys. Rev. B **76**, 024410 (2007).
[14] N. Magnani, A. Hiess, R. Caciuffo, E. Colineau, F. Wastin, J. Rebizant, and G. H. Lander, Phys. Rev. B **76**, 100404(R) (2007).
[15] D. Aoki, Y. Homma, Y. Shiokawa, E. Yamamoto, A. Nakamura, Y. Haga, R. Settai, and Y. Onuki, J. Phys. Soc. Jpn. **73**, 2608 (2004).
[16] I. Opahle, S. Elgazzar, V. D. P. Servedio, M. Richter, and P. M. Oppeneer, Europhys. Lett. **74**, 124 (2006).
[17] A. P. Hammersley, S. O. Svensson, M. Hanfland, A. N. Fitch, and D. Hausermann, High Press. Res. **14**, 235 (1996).
[18] P. S. Normile, S. Heathman, M. Idiri, P. Boulet, J. Rebizant, F. Wastin, G. H. Lander, T. Le Bihan, and A. Lindbaum, Phys. Rev. B **72**, 184508 (2005).
[19] J. Rodriguez-Carvajal, Physica B **55**, 192 (1993).
[20] F. Birch, J. Appl. Phys. **9**, 279 (1938).
[21] F. Birch, Phys. Rev. **71**, 809 (1947).
[22] F. D. Murnaghan, Am. J. Math. **59**, 235 (1937).
[23] H. Eschrig, M. Richter, and I. Opahle, in *Relativistic Electronic Structure Theory—Part II: Applications*, edited by P. Schwerdtfeger (Elsevier, Amsterdam, 2004), pp. 723–776.
[24] K. Koepernik and H. Eschrig, Phys. Rev. B **59**, 1743 (1999).
[25] J. P. Perdew and Y. Wang, Phys. Rev. B **45**, 13244 (1992).
[26] I. Opahle, S. Elgazzar, K. Koepernik, and P. M. Oppeneer, Phys. Rev. B **70**, 104504 (2004).
[27] I. Opahle and P. M. Oppeneer, Phys. Rev. Lett. **90**, 157001 (2003).
[28] A. B. Shick, V. Janiš, and P. M. Oppeneer, Phys. Rev. Lett. **94**, 016401 (2005).
[29] P. M. Oppeneer, A. B. Shick, J. Rusz, S. Lebègue, and O. Eriksson, J. Alloys Compd. **109**, 444 (2007).
[30] P. Söderlind, Phys. Rev. B **70**, 094515 (2004).